

Continuum strong-coupling expansion for quantum electrodynamics

Fred Cooper and Richard Kenway

Theoretical Division, Los Alamos National Laboratory, Los Alamos, New Mexico 87545

(Received 22 June 1981)

We derive from the path integral a continuum strong-coupling expansion for QED in d -dimensional Euclidean space-time. It is a double expansion in the fermion and boson kinetic energy (inverse free propagators), which leads to a double power series for the Green's functions of the cutoff theory in terms of $1/e^2$ and Λ^2/M^2 . Λ is a smooth cutoff in Euclidean momentum space, and M is an infrared regulator mass for the photons needed to define the local part of the path integral. We demonstrate how dimensional continuation is necessary to control the broken gauge invariance of the cutoff theory. Restricting to $d=2$ (the Schwinger model) we show how to remove the cutoff using Padé approximants. We find some evidence that as $\Lambda^2/M^2 \rightarrow \infty$ gauge invariance is restored and we calculate the vector-meson mass, keeping the first three terms in the expansion in powers of the bare photon inverse propagator.

I. INTRODUCTION

In a previous paper we have formulated a simple procedure for expanding the Green's functions of $g\phi^4$ field theory in d -dimensional space-time in inverse powers of the bare coupling.¹ We showed how to renormalize the lattice field theory and then take the continuum limit.²⁻⁴ Our approach was to treat the kinetic energy of the bosons as a perturbation, performing the path integration over the local self-interaction exactly. We used the lattice as a method of bounding the kinetic energy.

Gauge field theories, such as QED and QCD, present two difficulties not encountered in boson theories. The first difficulty is to find a lattice definition of the fermion inverse propagator that preserves chiral symmetry without changing the spectrum of states.⁵ We found by studying the strong-coupling expansion of the $(\bar{\psi}\psi)^2$ model in two dimensions that one way of circumventing this problem is to define the kinetic energy expansion in the continuum using a cutoff Λ to evaluate the momentum-space integrals. The parameter Λ was introduced by multiplying inverse propagators of momentum p by $\theta(\Lambda - |p|)$ and replaced the inverse lattice spacing of previous formulations. By doing this, state doubling was avoided and we obtained the correct mass gap in the large- N (number of species) limit of the model.⁶

The second potential problem is that our strong-coupling expansion (unlike that of Wilson^{5,7}) is based on treating interaction terms such as

$\bar{\psi}\gamma^\mu\psi A_\mu$ locally in the path integral and one wonders to what extent gauge invariance is destroyed by this assumption. The lesson learnt in weak-coupling perturbation theory is that one can consider $\bar{\psi}\gamma^\mu\psi A_\mu$ as a local interaction in some noninteger dimension d and preserve all the Ward identities. After renormalizing one then continues to the integer dimension of interest. This technique of dimensional continuation involves performing the coordinate or momentum space integrations in d -dimensional Euclidean space.^{8,9} As is well known, the method avoids all the intricacies of careful point splitting, needed to define gauge-invariant currents in integer dimensions. What we will show here is that a simple generalization of these ideas to the intrinsically divergent momentum-space integrals obtained in strong-coupling expansions seems to work in that, as the cutoff Λ is taken to infinity using Padé approximants, gauge invariance is restored. Technically, there is an approximate cancellation between poles and zeros at $d=2$ leaving a finite result for the photon mass.

In order to simplify our program of dimensional continuation for the continuum strong-coupling theory we use here a Gaussian cutoff in momentum space rather than a sharp θ -function cutoff. The Gaussian cutoff amounts to defining a regulated δ function in d -dimensional Euclidean space by

$$\delta_\Lambda(x) = (\Lambda^d/\pi^{d/2})e^{-\Lambda^2 x^2}. \quad (1.1)$$

(This is one of the cutoffs suggested by Castoldi

and Schomblond¹⁰; however these authors did not regulate the strong-coupling vertices correctly.¹¹ In Ref. 11 we compared the relative merits of the two continuum regulation schemes in the context of $g\phi^4$ field theory. The Gaussian has the advantage of leading to simple analytic forms (polynomials times exponentials) for the d -dimensional loop integrals. Its disadvantage is that it sometimes subtly ruins the ultraviolet behavior of certain Green's functions with the result that the sequence of approximants is only asymptotic. The θ -function scheme avoids these ultraviolet problems, but the multiloop integrals are more difficult (integrals over products of Bessel functions whose orders depend on the space-time dimension). For the interested reader this calculation in d dimensions is discussed in the Appendix. Since here we only

wish to demonstrate the feasibility of using dimensional continuation rather than to carry out extensive calculations, the simple analytic form obtained using a Gaussian cutoff is preferable and makes the results more transparent. It turns out that many of the strong-coupling diagrams are proportional to $(d-2)$ times powers of Λ . Thus we are not entitled to set $d=2$ before extrapolating to $\Lambda=\infty$. One sees that certain extrapolants generate approximate factors of $1/(d-2)$ which "cancel" the zeros at $d=2$, leaving finite answers.

Let us remind ourselves how weak-coupling dimensional continuation works in the solvable Schwinger model,¹² two-dimensional QED. The generating functional $Z[\bar{\eta}, \eta, J_\mu]$ for QED in a general α gauge in d -dimensional Euclidean space is

$$Z[\bar{\eta}, \eta, J_\mu] = N \int D\bar{\psi} D\psi DA_\mu \exp \left[- \int d^d x [\bar{\psi} S^{-1} \psi - A_\mu D^{-1}_{\mu\nu}(\alpha) A_\nu + ie \bar{\psi} \not{A} \psi + J_\mu A_\mu + \bar{\psi} \eta + \bar{\eta} \psi] \right], \quad (1.2)$$

where

$$S^{-1}(x-y) \equiv \not{\partial} \delta(x-y), \quad (1.3a)$$

$$D_{\mu\nu}^{-1}(\alpha; x-y) \equiv [\delta_{\mu\nu} \partial^2 - (1-1/\alpha) \partial_\mu \partial_\nu] \delta(x-y). \quad (1.3b)$$

Performing the path integration over $\bar{\psi}$ and ψ gives

$$\begin{aligned} Z[\bar{\eta}, \eta, J_\mu] &= N \int DA_\mu \exp \left[\int d^d x \text{Tr} \ln(\not{\partial} + ie \not{A}) \right] \exp \left[\int d^d x \left[\bar{\eta} \frac{1}{\not{\partial} + ie \not{A}} \eta + A_\mu D^{-1}_{\mu\nu} A_\nu - J_\mu A_\mu \right] \right] \\ &= N' \int DA_\mu \exp \left[\int d^d x \text{Tr} \ln(1 + ie \not{A} S) \right] \exp \left[\int d^d x \left[\bar{\eta} \frac{1}{\not{\partial} + ie \not{A}} \eta + A_\mu D^{-1}_{\mu\nu} A_\nu - J_\mu A_\mu \right] \right]. \end{aligned} \quad (1.4)$$

The expansion of $\ln(1 + ie \not{A} S)$ gives the sum of all single-loop fermion diagrams with n external photons A_μ . The reason the Schwinger model is solvable is a property of γ matrices, namely,

$$\gamma_\mu \not{A} \gamma_\mu = (2-d) \not{A}, \quad (1.5)$$

so that all finite terms in the expansion of the logarithm vanish. The only term which does not automatically vanish is the vacuum polarization, since it is intrinsically divergent. The correct gauge-invariant answer for $A_\mu(x) \Pi_{\mu\nu}(x,y) A_\nu(y)$ is obtained using dimensional continuation or by point splitting. Naively one has

$$\Pi_{\mu\nu}(x,y) = e^2 \text{Tr} \gamma_\mu S(x-y) \gamma_\nu S(y-x) \quad (1.6a)$$

and

$$\Pi_{\mu\nu}(p) = e^2 \int \frac{d^2 q}{(2\pi)^2} \frac{\text{Tr} \gamma_\mu \not{q} \gamma_\nu (\not{q} - \not{p})}{q^2 (q-p)^2}. \quad (1.6b)$$

We notice that $\Pi_{\mu\nu} \propto (2-d)$ times an integral which diverges in two dimensions. So one cannot obtain the correct answer for $\Pi_{\mu\nu}$ from Eq. (1.6b). By point splitting one finds that $\Pi_{\mu\nu}$ is not given correctly by (1.6) in either two or four dimensions. This approach is discussed extensively by Schwinger and Johnson^{12,13} and is the basis for Wilson's gauge-invariant approach to lattice gauge field theories. However, if we redefine

$\Pi_{\mu\nu}(p)$ as follows,⁹

$$\begin{aligned}\Pi_{\mu\nu}(p) &= e^2 \int \frac{d^d q}{(2\pi)^d} \frac{\text{Tr} \gamma_\mu \not{q} \gamma_\nu (\not{q} - \not{p})}{q^2 (q-p)^2} \\ &= \frac{2^{d/2}}{(4\pi)^{d/2}} e^2 \int_0^1 dx \frac{\Gamma(2-d/2)}{[p^2(x-x^2)]^{2-d/2}} 2(\delta_{\mu\nu} p^2 - p_\mu p_\nu)(x-x^2),\end{aligned}\quad (1.7)$$

then letting $d \rightarrow 2$ we get

$$\Pi_{\mu\nu}(p) = (e^2/\pi)(\delta_{\mu\nu} - p_\mu p_\nu/p^2) \quad (1.8)$$

which is the correct answer and leads immediately to the result that the exact photon propagator is

$$D_{\mu\nu}(p) = \frac{\delta_{\mu\nu} - p_\mu p_\nu/p^2}{p^2 + e^2/\pi} + \alpha \frac{p_\mu p_\nu}{p^4}. \quad (1.9)$$

Let us look closely to see what has canceled the factor of $d-2$ when we calculate in d dimensions. From (1.7),

$$\Pi_{\mu\mu}(p) = e^2 \int \frac{d^d q}{(2\pi)^d} \frac{2^{d/2}(2-d)(q^2 - p \cdot q)}{q^2 (q-p)^2}. \quad (1.10)$$

Introducing Feynman parameters and using standard d -dimensional integrals,

$$\int \frac{d^d q}{(2\pi)^d} \frac{1}{(q^2 + 2k \cdot q + \Lambda)^\alpha} = \frac{1}{(4\pi)^{d/2} (\Lambda - k^2)^{\alpha-d/2}} \frac{\Gamma(\alpha-d/2)}{\Gamma(\alpha)}, \quad (1.11)$$

we obtain

$$\Pi_{\mu\mu}(p) = e^2 \frac{2^{d/2}}{(4\pi)^{d/2}} \int_0^1 dx \frac{\Gamma(2-d/2)(2-d)p^2(x-x^2)}{[p^2(x-x^2)]^{2-d/2}} \left[\frac{d}{2} \frac{\Gamma(1-d/2)}{\Gamma(2-d/2)} - 1 \right]. \quad (1.12)$$

Thus, we see that the zero $(2-d)$ is canceled by the pole in $\Gamma(1-d/2)$ at $d=2$, since $(1-d/2)\Gamma(1-d/2) = \Gamma(2-d/2) \rightarrow 1$ as $d \rightarrow 2$, and

$$\Pi_{\mu\mu}(p) \xrightarrow{d \rightarrow 2} e^2/\pi. \quad (1.13)$$

Hence the dimensionally continued expression for $\Pi_{\mu\mu}(p)$, Eq. (1.10), develops the correct singularity at $d=2$ to cancel the factor of $(d-2)$ from the trace over γ matrices and give the correct gauge-invariant answer.

We will find that many terms in the strong-coupling expansion of $\Pi_{\mu\mu}$ also are proportional to $(d-2)$. However, they are multiplied by positive powers of Λ . If we kept Λ finite and let $d \rightarrow 2$ ignoring these terms, we would get the wrong answer. After extrapolating to $\Lambda \rightarrow \infty$, we find there are many zeros and poles near two dimensions. By assuming that the zeros and poles are actually at $d=2$, these singularities cancel and we obtain a reasonable result for the photon mass.

The outline of the rest of this paper is as follows. In Sec. II we derive the generating functional for the strong-coupling expansion for d -dimensional

QED by explicitly performing the integrals for the local part of the theory and explain how to obtain a finite continuum formulation. In Sec. III we give the rules for evaluating strong-coupling diagrams in terms of the infinite number of vertices of the local theory and the bare inverse propagators $S^{-1}(x,y)$, $D^{-1}_{\mu\nu}(x,y)$. In Sec. IV we evaluate the photon propagator as a double power series in $1/e^2$ and Λ^2/M^2 , where M is an infrared regulator mass. Using Padé extrapolants we show that, as Λ^2/M^2 goes to infinity, gauge invariance is restored in the subclass of graphs having no fermion loops and we obtain a reasonable photon mass $3e/\sqrt{\pi}$ by including terms up to $(\Lambda^2/M^2)^2$. In the Appendix we discuss how to evaluate strong-coupling diagrams using both the Gaussian and θ -function regulated δ function.

II. THE GENERATING FUNCTIONAL FOR THE STRONG-COUPLED EXPANSION

The Euclidean form of the generating functional for d -dimensional QED is

$$Z_d = \int D\bar{\psi}D\psi DA_\mu \exp \left[- \int d^d x L_E \right], \quad (2.1)$$

$$L_E = (F_{\mu\nu})^2/4 + M^2 A^2/2 + \bar{\psi}(\not{\partial} + ie\not{A})\psi, \quad (2.2)$$

where

$$F_{\mu\nu} = \partial_\mu A_\nu - \partial_\nu A_\mu, \quad (2.3)$$

$$\not{A} = A_\mu \gamma_\mu, \quad (2.4)$$

and the Euclidean γ matrices obey

$$\{\gamma_\mu, \gamma_\nu\} = 2\delta_{\mu\nu}. \quad (2.5)$$

It is necessary to introduce a photon mass in order to regulate the photon part of the strong-coupling expansion. (Physically, expansion about a static limit for massless particles is nonsensical.) Its introduction eliminates the explicit need for a gauge-fixing term, i.e. it selects the $\alpha = \infty$ Lorentz gauge. However, it is useful to work in a general covariant gauge in order to be able to check the α dependence of the calculation. We will show how the $M \rightarrow 0$ limit may be ultimately taken after the cutoff is removed (see Sec. IV).

The photon and fermion kinetic energies are extracted via¹

$$Z_d[\bar{\eta}, \eta, J_\mu] = K_A K_\psi \int D\bar{\psi}D\psi DA_\mu \exp \left[- \int d^d x \left(\frac{1}{2} M^2 A^2 + ie\bar{\psi}\not{A}\psi + J_\mu A_\mu + \bar{\psi}\eta + \bar{\eta}\psi \right) \right], \quad (2.6)$$

where, in a general covariant gauge ($g = 1 - 1/\alpha$),

$$K_A \equiv \exp \left[\frac{1}{2} \int d^d x d^d y [\delta/\delta J_\mu(x)] D^{-1}_{\mu\nu}(x,y) [\delta/\delta J_\nu(y)] \right], \quad (2.7a)$$

$$D^{-1}_{\mu\nu}(x,y) = (\delta_{\mu\nu} \partial^2 - g \partial_\mu \partial_\nu) \delta(x-y) \quad (2.7b)$$

and

$$K_\psi \equiv \exp \left[- \int d^d x d^d y [\delta/\delta \eta(x)] S^{-1}(x,y) [\delta/\delta \bar{\eta}(y)] \right], \quad (2.8a)$$

$$S^{-1}(x,y) = \not{\partial} \delta(x-y). \quad (2.8b)$$

The remaining functional integral in Eq. (2.6) is a product of one-dimensional integrals at each space-time point. Formally, space-time is divided into cells of volume $\delta_\Lambda(0)^{-1}$, with an appropriate choice for the regulation of the δ function. In this paper we use the Gaussian cutoff, Eq. (1.1), so that the volume of the unit cell is

$$\delta_\Lambda(0)^{-1} = \pi^{d/2} / \Lambda^d. \quad (2.9)$$

An alternative is the sharp momentum cutoff discussed in the Appendix. This definition (1.1) simultaneously regulates the highly singular inverse propagators (2.7b) and (2.8b). In coordinate space they become

$$D^{-1}_{\mu\nu}(x,0;\Lambda) = 2\Lambda^2 \delta_\Lambda(0) [2\Lambda^2 (\delta_{\mu\nu} x^2 - g x_\mu x_\nu) + (g-d)\delta_{\mu\nu}] e^{-\Lambda^2 x^2}, \quad (2.10a)$$

$$S^{-1}(x,0;\Lambda) = -2\Lambda^2 \delta_\Lambda(0) \not{x} e^{-\Lambda^2 x^2} \quad (2.10b)$$

and in momentum space

$$D^{-1}_{\mu\nu}(p;\Lambda) = (g p_\mu p_\nu - \delta_{\mu\nu} p^2) e^{-p^2/4\Lambda^2}, \quad (2.11a)$$

$$S^{-1}(p;\Lambda) = i\not{p} e^{-p^2/4\Lambda^2}. \quad (2.11b)$$

In a previous paper it was shown how the step-function continuum regulation of $S^{-1}(p;\Lambda) = i\not{p} \theta(\Lambda - |p|)$ avoids fermion species doubling.⁶ Equation (2.11b) shares this feature. Also, we observe that Eq. (2.11a) has the correct rotational invariance which would be destroyed by going onto a lattice.

The result of the fermion integration in Eq. (2.6) is formally

$$Z_d[\bar{\eta}, \eta, J_\mu] = K_A K_\psi \int DA_\mu \exp \left[- \int d^d x \left[(i/e)\bar{\eta}\not{A}^{-1}\eta - (d/2)\delta_\Lambda(0) \ln(-e^2 A^2) + \frac{1}{2} M^2 A^2 + J_\mu A_\mu \right] \right]. \quad (2.12)$$

In order to carry out the gauge-field integration we split it into a product of d -dimensional integrals at each

space-time point \underline{n} , labeling a volume $\delta_\Lambda(0)^{-1}$, so that $\int d^d x = \delta_\Lambda(0)^{-1} \sum_{\underline{n}}$. Then

$$Z_d[\bar{\eta}, \eta, J_\mu] = K_A K_\psi \prod_{\underline{n}} \left\{ \int d^d A_{\underline{n}} (-e^2 A_{\underline{n}}^2)^{d/2} \exp \left[\frac{-i}{e \delta_\Lambda(0)} \frac{\bar{\eta}_{\underline{n}} \not{A}_{\underline{n}} \eta_{\underline{n}}}{A_{\underline{n}}^2} \right] \exp \left[-\frac{M^2 A_{\underline{n}}^2}{2 \delta_\Lambda(0)} - \frac{J_{\mu \underline{n}} A_{\mu \underline{n}}}{\delta_\Lambda(0)} \right] \right\}. \quad (2.13)$$

Here we have used $\not{A}_{\underline{n}}^2 = A_{\underline{n}}^2$, which follows directly from Eq. (2.5), to simplify the fermion source term. The integrand can be simplified by recognizing that the expansion of the exponential of the fermion sources truncates after d terms, because of the Pauli principle. Thus, in two dimensions,

$$Z_2[\bar{\eta}, \eta, J_\mu] = K_A K_\psi \prod_{\underline{n}} \left\{ \int d^2 A_{\underline{n}} (-e^2 A_{\underline{n}}^2) \left[1 - \frac{i}{e \delta_\Lambda(0)} \frac{\bar{\eta}_{\underline{n}} \not{A}_{\underline{n}} \eta_{\underline{n}}}{A_{\underline{n}}^2} - \frac{1}{2e^2 \delta_\Lambda(0)^2} \left(\frac{\bar{\eta}_{\underline{n}} \not{A}_{\underline{n}} \eta_{\underline{n}}}{A_{\underline{n}}^2} \right)^2 \right] \right. \\ \left. \times \exp \left[-\frac{M^2 A_{\underline{n}}^2}{2 \delta_\Lambda(0)} - \frac{J_{\mu \underline{n}} A_{\mu \underline{n}}}{\delta_\Lambda(0)} \right] \right\} \quad (2.14)$$

and again we are helped by the truncation of local products of fermion sources, since

$$(\bar{\eta} \not{A} \eta)^2 = \frac{1}{2} A^2 (\bar{\eta} \gamma_\mu \eta)^2 \quad (d=2) \quad (2.15)$$

so that

$$Z_2[\bar{\eta}, \eta, J_\mu] = K_A K_\psi \prod_{\underline{n}} \left\{ \int d^2 A_{\underline{n}} \left[A_{\underline{n}}^2 - \frac{i}{e \delta_\Lambda(0)} \bar{\eta}_{\underline{n}} A_{\underline{n}} \eta_{\underline{n}} - \frac{1}{4e^2 \delta_\Lambda(0)^2} (\bar{\eta}_{\underline{n}} \gamma_\mu \eta_{\underline{n}})^2 \right] \exp \left[-\frac{M^2 A_{\underline{n}}^2}{2 \delta_\Lambda(0)} - \frac{J_{\mu \underline{n}} A_{\mu \underline{n}}}{\delta_\Lambda(0)} \right] \right\} \\ = K_A K_\psi \prod_{\underline{n}} \left\{ \left[\delta_\Lambda(0)^2 \left(\frac{\partial}{\partial J_{\mu \underline{n}}} \right)^2 + (i/e) \bar{\eta}_{\underline{n}} \gamma_\mu \eta_{\underline{n}} \frac{\partial}{\partial J_{\mu \underline{n}}} - \frac{1}{4e^2 \delta_\Lambda(0)^2} (\bar{\eta}_{\underline{n}} \gamma_\mu \eta_{\underline{n}})^2 \right] \exp \left[\frac{J_{\underline{n}}^2}{2M^2 \delta_\Lambda(0)} \right] \right\} \\ = K_A K_\psi \prod_{\underline{n}} \left\{ \left[\frac{2\delta_\Lambda(0)}{M^2} + \frac{J_{\underline{n}}^2}{M^4} + \frac{i}{e \delta_\Lambda(0) M^2} \bar{\eta}_{\underline{n}} \not{J}_{\underline{n}} \eta_{\underline{n}} - \frac{1}{4e^2 \delta_\Lambda(0)^2} (\bar{\eta}_{\underline{n}} \gamma_\mu \eta_{\underline{n}})^2 \right] \exp \left[\frac{J_{\underline{n}}^2}{2M^2 \delta_\Lambda(0)} \right] \right\} \quad (2.16)$$

ignoring changes in the normalization of Z_2 . The vertices of the strong-coupling theory are obtained by reexponentiating. As discussed in Ref. 11 the correct identification of lattice with continuum sources is

$$\eta_{\underline{n}} \rightarrow \eta_s(x) \equiv \int d^d z \delta_\Lambda(x-z) \eta(z), \quad (2.17)$$

etc., where the regulated δ function is defined in Eq. (1.1). Smearing of continuum sources is necessary to ensure that the theory without kinetic energy is finite. The result is

$$Z_2[\bar{\eta}, \eta, J_\mu] = K_A K_\psi \exp \left\{ \int d^2 x \left[\frac{J_s^2}{2M^2} + \delta_\Lambda(0) \ln \left[1 + \frac{J_s^2}{2M^2 \delta_\Lambda(0)} \right] \right] \right\} \\ \times \exp \left\{ \int d^2 x \left[\frac{i}{2e \delta_\Lambda(0)} \frac{\bar{\eta}_s \not{J}_s \eta_s}{[1 + J_s^2/2M^2 \delta_\Lambda(0)]} - \frac{M^2}{8e^2 \delta_\Lambda(0)^2} \frac{(\bar{\eta}_s \gamma_\mu \eta_s)^2}{[1 + J_s^2/2M^2 \delta_\Lambda(0)]^2} \right] \right\}. \quad (2.18)$$

All Green's functions of the two-dimensional theory can be obtained from (2.18) by functional differentiation. We use it to determine the strong-coupling Feynman rules in the next section.

Before doing so, we mention how the preceding analysis can be carried out in four dimensions. Expanding the exponential of the fermion source term in (2.13) for $d=4$, we find

$$Z_4[\bar{\eta}, \eta, J_\mu] = K_A K_\psi \prod_n \left\{ \int d^4 A_n \left[(A_n^2)^2 - \frac{i}{e\delta_\Lambda(0)} A_n^2 \bar{\eta}_n \not{A}_n \eta_n - \frac{1}{2e^2 \delta_\Lambda(0)^2} (\bar{\eta}_n \not{A}_n \eta_n)^2 \right. \right. \\ \left. \left. + \frac{i}{6e^3 \delta_\Lambda(0)^3} \frac{(\bar{\eta}_n \not{A}_n \eta_n)^3}{A_n^2} + \frac{1}{24e^4 \delta_\Lambda(0)^4} \frac{(\bar{\eta}_n \not{A}_n \eta_n)^4}{A_n^2} \right] \right. \\ \left. \times \exp \left[-\frac{M^2 A_n^2}{2\delta_\Lambda(0)} - \frac{J_{\mu n} A_{\mu n}}{\delta_\Lambda(0)} \right] \right\}. \quad (2.19)$$

Two truncation theorems analogous to (2.15) are helpful here,

$$(\bar{\eta} \not{A} \eta)^3 = \frac{1}{2} A^2 (\bar{\eta} \not{A} \eta) (\bar{\eta} \gamma_\mu \eta)^2 \quad (d=4) \quad (2.20)$$

and

$$(\bar{\eta} \not{A} \eta)^4 = \frac{1}{8} (A^2)^2 [(\bar{\eta} \gamma_\mu \eta)^2]^2 \quad (d=4). \quad (2.21)$$

So, as in two dimensions, the powers of A^2 in the denominators in Eq. (2.19) are canceled, leaving gauge-field integrations which can be carried out in the same way as in (2.16). The result after smearing continuum sources is

$$Z_4[\bar{\eta}, \eta, J_\mu] = K_A K_\psi \exp \left\{ \int d^4 x \left[\frac{J_s^2}{2M^2} + \delta_\Lambda(0) \ln \left[1 + \frac{J_s^2}{2M^2 \delta_\Lambda(0)} + \frac{(J_s^2)^2}{24M^4 \delta_\Lambda(0)^2} \right] \right] \right\} \\ \times \exp \left\{ \int d^4 x \left[\frac{i}{4e\delta_\Lambda(0)} \frac{[1 + J_s^2/6M^2 \delta_\Lambda(0)]}{[1 + J_s^2/2M^2 \delta_\Lambda(0) + (J_s^2)^2/24M^4 \delta_\Lambda(0)^2]} \bar{\eta}_s \not{J}_s \eta_s \right. \right. \\ \left. \left. - \frac{M^2}{48e^2 \delta_\Lambda(0)^2} \frac{(\bar{\eta}_s \gamma_\mu \eta_s)^2}{[1 + J_s^2/2M^2 \delta_\Lambda(0) + (J_s^2)^2/24M^4 \delta_\Lambda(0)^2]} \right. \right. \\ \left. \left. + \frac{1}{96e^2 \delta_\Lambda(0)^3} \frac{(\bar{\eta}_s \not{J}_s \eta_s)^2}{[1 + J_s^2/2M^2 \delta_\Lambda(0) + (J_s^2)^2/24M^4 \delta_\Lambda(0)^2]^2} \right. \right. \\ \left. \left. + \frac{iM^2}{576e^3 \delta_\Lambda(0)^4} \frac{[1 - (J_s^2)^2/24M^4 \delta_\Lambda(0)^2]}{[1 + J_s^2/2M^2 \delta_\Lambda(0) + (J_s^2)^2/24M^4 \delta_\Lambda(0)^2]^3} (\bar{\eta}_s \gamma_\mu \eta_s)^2 (\bar{\eta}_s \not{J}_s \eta_s) \right. \right. \\ \left. \left. + \frac{M^2 J_s^2}{9216e^4 \delta_\Lambda(0)^6} \frac{[1 + 3J_s^2/8M^2 \delta_\Lambda(0) - (J_s^2)^2/24M^2 \delta_\Lambda(0)^2]}{[1 + J_s^2/2M^2 \delta_\Lambda(0) + (J_s^2)^2/24M^2 \delta_\Lambda(0)^2]^4} [(\bar{\eta}_s \gamma_\mu \eta_s)^2]^2 \right] \right\}. \quad (2.22)$$

The strong-coupling diagram rules may be read directly from Eq. (2.22). For the remainder of this paper we shall be concerned with the two-dimensional theory, Eq. (2.18). Our aim is to indicate how gauge invariance is restored as the cutoff is removed and why a strong-coupling version of dimensional continuation is needed. The example we use is a calculation of the photon mass.

III. DIAGRAM RULES AND THE PHOTON PROPAGATOR

As formulated in Eq. (2.18) the Green's functions of the Schwinger model may be calculated as a double expansion in the inverse fermion and photon propagators. These are the lines of our strong-coupling diagrams (see Fig. 1). There is an

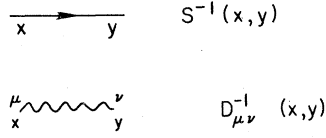


FIG. 1. Lines of the strong-coupling expansion. $S^{-1}(x, y) = \not{\partial} \delta(x - y)$, $D_{\mu\nu}^{-1}(x, y) = (\delta_{\mu\nu} \partial^2 - g \partial_\mu \partial_\nu) \times \delta(x - y)$.

infinite number of vertices, a typical feature of strong-coupling expansions, and they fall into the three types shown in Fig. 2. In order to reduce the complexity somewhat we focus on the full propagator $D_{\mu\nu}(k)$ of a photon of momentum k .

Let $\Pi_{\mu\nu}^{-1}(k; \Lambda)$ be the sum of all one-particle irreducible (1PI) diagrams (in terms of inverse propagators) with two external photon legs, carrying momentum k . Then, in general,

$$\Pi_{\mu\nu}^{-1}(k; \Lambda) = A(k^2, \Lambda^2, M^2) \delta_{\mu\nu} + B(k^2, \Lambda^2, M^2) k_\mu k_\nu, \quad (3.1)$$

where A and B are polynomials times exponentials in k^2 (since no inverse powers of k^2 are allowed by the strong-coupling expansion). They are also functions of Λ^2 , M^2 , and e^2 . Graphically, this inverse self-energy can be organized into an expansion in inverse powers of e^2 :

$$\Pi_{\mu\nu}^{-1}(k; \Lambda) = \sum_{n=0}^{\infty} (1/e^{2n}) \Pi_{\mu\nu}^{(n)-1}(k; \Lambda), \quad (3.2)$$

where the graphs contributing to each of the coefficients are shown in Fig. 3. The result of smearing the vertices in Eq. (2.18) is that the inverse free propagators for each internal line, Eq. (2.11), get replaced by

$$D^{-1}_{\mu\nu}(k; \Lambda) \rightarrow \tilde{D}^{-1}_{\mu\nu}(k; \Lambda) = \delta_{\Lambda}(k)^2 D^{-1}_{\mu\nu}(k; \Lambda), \quad (3.3a)$$

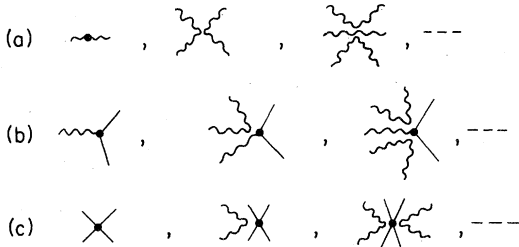


FIG. 2. Vertices of QED ($d=2$): (a) purely photonic vertices; (b) vertices with two fermions and an odd number of photons; (c) vertices with four fermions and an even number of photons.

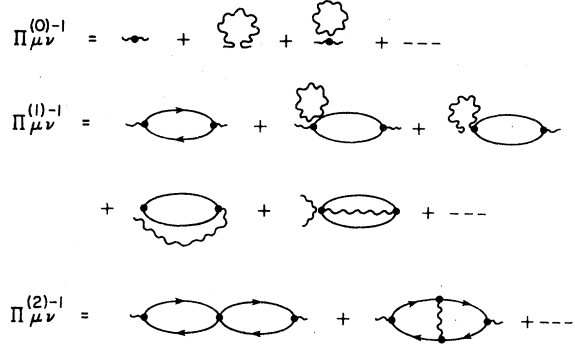


FIG. 3. Graphs in the expansion of $\Pi_{\mu\nu}^{-1}(k, \Lambda)$ [see Eq. (3.2)].

$$S^{-1}(k; \Lambda) \rightarrow \tilde{S}^{-1}(k; \Lambda) = \delta_{\Lambda}(k)^2 S^{-1}(k; \Lambda) \quad (3.3b)$$

if we use the formal local vertices of the theory.¹¹ In addition there is an overall factor of $\delta_{\Lambda}(k)^2$ from the two external legs of $\Pi_{\mu\nu}^{-1}$. So writing

$$\Pi_{\mu\nu}^{-1}(k; \Lambda) = \delta_{\Lambda}(k)^2 \tilde{\Pi}_{\mu\nu}^{-1}(k; \Lambda), \quad (3.4)$$

where $\tilde{\Pi}_{\mu\nu}^{-1}$ is 1PI in $\tilde{D}_{\mu\nu}^{-1}$ and \tilde{S}^{-1} and is calculated using the local vertices, the full photon propagator obeys the Dyson equation (see Fig. 4)

$$D_{\mu\nu}(k; \Lambda) = \delta_{\Lambda}(k)^2 \tilde{\Pi}_{\mu\nu}^{-1}(k; \Lambda) + \tilde{\Pi}_{\mu\rho}^{-1}(k; \Lambda) \tilde{D}_{\rho\sigma}^{-1}(k; \Lambda) D_{\sigma\nu}(k; \Lambda). \quad (3.5)$$

Decomposing into transverse and longitudinal parts via

$$f_{\mu\nu}(k) \equiv f_T(k) (\delta_{\mu\nu} - k_\mu k_\nu / k^2) + f_L(k) k_\mu k_\nu / k^2 \quad (3.6)$$

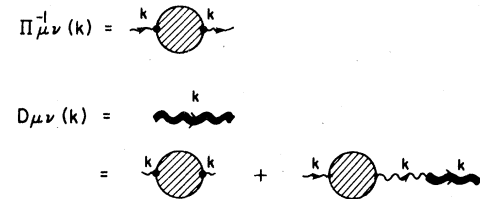


FIG. 4. Schwinger-Dyson equation for the full photon propagator. The full wavy line is the full propagator $D_{\mu\nu}$. The light wavy line is the bare inverse propagator $D_{\mu\nu}^{-1(0)}$. The blob is $\Pi_{\mu\nu}^{-1}(k, \Lambda)$.

we have

$$\begin{aligned} D_T(k; \Lambda) &= \frac{\delta_\Lambda(k^2)}{\tilde{\Pi}_T(k; \Lambda) - \tilde{D}_T^{-1}(k; \Lambda)} \\ &= \frac{\delta_\Lambda(k)^2}{k^2 \delta_\Lambda(k)^3 + \tilde{\Pi}_T(k; \Lambda)} \end{aligned} \quad (3.7)$$

and

$$\begin{aligned} D_L(k; \Lambda) &= \frac{\delta_\Lambda(k)^2}{\tilde{\Pi}_L(k; \Lambda) - \tilde{D}_L^{-1}(k; \Lambda)} \\ &= \frac{\delta_\Lambda(k)^2}{(k^2/\alpha) \delta_\Lambda(k)^3 + \tilde{\Pi}_L(k; \Lambda)} \end{aligned} \quad (3.8)$$

Thus we see that $\tilde{\Pi}_{\mu\nu}(k; \Lambda)$ is the usual vacuum polarization as $\Lambda \rightarrow \infty$. Explicitly, with the Gaussian regulation scheme,

$$\begin{aligned} D_{\mu\nu}(k; \Lambda) &= \frac{e^{-k^2/2\Lambda^2} (\delta_{\mu\nu} - k_\mu k_\nu / k^2)}{k^2 e^{-3k^2/4\Lambda^2} + \tilde{\Pi}_T(k; \Lambda)} \\ &\quad + \frac{e^{-k^2/2\Lambda^2} k_\mu k_\nu / k^2}{(k^2/\alpha) e^{-3k^2/4\Lambda^2} + \tilde{\Pi}_L(k; \Lambda)}. \end{aligned} \quad (3.9)$$

This is to be compared with the exact result for the Schwinger model for $\alpha = \infty$ in the limit $\Lambda \rightarrow \infty$,

$$D_{\mu\nu}(k) = \frac{\delta_{\mu\nu} - k_\mu k_\nu / k^2}{M^2 + e^2/\pi + k^2} + \frac{k_\mu k_\nu}{M^2 k^2}. \quad (3.10)$$

Thus, we deduce that, after removal of the cutoff,

$$\begin{aligned} \tilde{\Pi}_{\mu\nu}^{-1}(k) &= \Pi_{\mu\nu}^{-1}(k) \\ &= \frac{\delta_{\mu\nu} - k_\mu k_\nu / k^2}{M^2 + e^2/\pi} + \frac{k_\mu k_\nu}{M^2 k^2} \end{aligned} \quad (3.11)$$

which has a strong-coupling expansion

$$\begin{aligned} \Pi_{\mu\nu}^{-1}(k) &= \frac{k_\mu k_\nu}{M^2 k^2} + (\pi/e^2) (\delta_{\mu\nu} - k_\mu k_\nu / k^2) \\ &\quad \times \sum_{n=0}^{\infty} (-1)^n (\pi M^2 / e^2)^n. \end{aligned} \quad (3.12)$$

In what follows we shall concentrate on $\Pi_{\mu\mu}^{-1}$ which has the strong-coupling expansion

$$\Pi_{\mu\mu}^{-1} = 1/M^2 + (\pi/e^2) \sum_{n=0}^{\infty} (-1)^n (\pi M^2 / e^2)^n. \quad (3.13)$$

The Λ -regulated expansion is given in Eq. (3.2) and this can only agree with Eq. (3.13) if, in the limit $\Lambda^2/M^2 \rightarrow \infty$,

$$\begin{aligned} \Pi_{\mu\mu}^{(0)-1} &\rightarrow 1/M^2, \\ \Pi_{\mu\mu}^{(n)-1} &\rightarrow \pi (-1)^{n-1} (\pi M^2)^{n-1} \quad (n \geq 1). \end{aligned} \quad (3.14)$$

To the order we calculate (Λ^6/M^6) almost all the diagrams contributing to the $1/M^2$ term in Eq. (3.13) are proportional to $\delta_{\mu\nu}/M^2$ and not $k_\mu k_\nu/M^2$ (see Fig. 7, where only the last two diagrams contribute to $k_\mu k_\nu/M^2$) and we expect them to vanish as the cutoff is removed since they are not present in Eq. (3.12). These nonzero and α -dependent contributions to $\Pi_{\mu\nu}^{(0)-1}$ in the cutoff theory are a consequence of our violation of gauge invariance. Hence, we regard the rate at which the extrapolants for $\Pi_{\mu\mu}^{(0)-1}$ vanish and become α -independent as a test of how well gauge invariance is restored, order by order in the strong-coupling expansion, as the cutoff is removed. In addition, we wish to show that the extrapolants for $\Pi_{\mu\mu}^{(1)-1}$ are approaching π .

The diagram rules for $\Pi_{\mu\nu}^{(0)-1}$ and $\Pi_{\mu\nu}^{(1)-1}$ are obtained directly from Eq. (2.18). We need keep only one fermion loop and consider the reduced generating functional for dimension $d \leq 2$, obtained by expanding Eq. (2.18) in inverse powers of e and carrying out the fermionic functional differentiation

$$\begin{aligned} Z'[J_\mu] &= K_A \exp \left\{ \int d^d x \left[J_s^2 / (2M^2) + \delta_\Lambda(0) \ln \left(1 + \frac{J_s^2}{2M^2 \delta_\Lambda(0)} \right) \right] \right\} \\ &\quad \times \left[1 + \frac{1}{8e^2 \delta_\Lambda(0)^2} \int d^d x d^d y \frac{J_{s\mu}(x) J_{s\nu}(y) \text{Tr}[\gamma_\mu \tilde{S}^{-1}(x, y) \gamma_\nu \tilde{S}^{-1}(y, x)]}{[1 + J_s(x)^2 / 2M^2 \delta_\Lambda(0)][1 + J_s(y)^2 / 2M^2 \delta_\Lambda(0)]} \right]. \end{aligned} \quad (3.15)$$

Then all topologically distinct 1PI diagrams with zero or one fermion loop are drawn and evaluated as follows.

1. Photons only ($\Pi_{\mu\nu}^{(0)-1}$)

(a) Vertices may have any even number of photon legs; a vertex with $2l$ legs carries a weight v_{2l} given by

$$\begin{aligned}
 & J^2/2M^2 + \delta_\Lambda(0) \ln \left[1 + \frac{J^2}{2M^2\delta_\Lambda(0)} \right] \\
 & \equiv \sum_{l=1}^{\infty} v_{2l}(J^2)^l \\
 & = J^2/2M^2 + \sum_{l=1}^{\infty} \frac{(-1)^{l-1}}{l} \frac{\delta_\Lambda(0)}{(2M^2\delta_\Lambda(0))^l} (J^2)^l
 \end{aligned} \tag{3.16}$$

together with a factor

$$\prod_{i=1}^{2l} \delta_\Lambda(p_i) \delta \left[\sum_{i=1}^{2l} p_i \right]$$

where p_i is the momentum in the i th leg. The first few are shown in Fig. 5.

(b) In any given diagram, if there are m_1 vertices of type 1, m_2 vertices of type 2, etc., divide by $m_1!m_2! \dots$

(c) Join the vertices of a diagram in all possible ways using the photon lines of Fig. 1 ignoring direction and Lorentz indices. Count the number of ways of attaching the external legs and multiply by the number of ways of joining up the remaining legs of each vertex. Multiply the value of the diagram by this counting factor.

2. One fermion loop ($\Pi_{\mu\nu}^{(1)-1}$)

(a) Some of the new vertices are shown in Fig. 6. Each end of the fermion loop may have any odd

$$\begin{aligned}
 \text{---} \bullet \text{---} &= \frac{1}{M^2} \\
 \text{---} \times \text{---} &= -\frac{1}{8M^4 \delta_d(0)} \\
 \text{---} \times \times \text{---} &= \frac{1}{24M^6 \delta_d(0)^2}
 \end{aligned}$$

FIG. 5. Photonic vertices with two, four, and six legs. Note that these vertices are proportional to $M^{-2\kappa}$ where 2κ is the number of legs.

number of photon legs; a loop with $2k + 1$ photon legs at one end and $2l + 1$ at the other carries a weight $f_{k,l}$ given by

$$\begin{aligned}
 & \frac{1}{8\delta_\Lambda(0)^2} \left[1 + \frac{J(x)^2}{2M^2\delta_\Lambda(0)} \right]^{-1} \left[1 + \frac{J(y)^2}{2M^2\delta_\Lambda(0)} \right]^{-1} \\
 & = \sum_{k,l=0}^{\infty} f_{k,l} [J(x)^2]^k [J(y)^2]^l.
 \end{aligned} \tag{3.17}$$

At each end of the fermion loop there is a momentum-conserving δ function and a factor $\delta_\Lambda(p)$ for each line of momentum p .

(b) There is only one new vertex, the fermion loop, so there is no change in the combinatorial factor from that in 1(b).

(c) Calculate the counting factor as in 1(c), treating the fermion loop as a new photon vertex.

3. Evaluation of diagrams

(a) Take the product of the inverse propagators (Fig. 1) and vertices for a given diagram, contracting Lorentz indices at each vertex.

(b) Integrate over all internal space-time points.

We notice from Eq. (3.15) that each internal fermion line carries with it a factor of $1/e$ and each internal photon line carries a factor $[M^2\delta_\Lambda(0)]^{-1}$. Thus, the strong-coupling expansion for the Λ -regulated theory is a double power series in $1/e$ and Λ^2/M^2 .

IV. CALCULATION OF THE PHOTON MASS

In this section we wish to calculate the photon mass and show that gauge-dependent terms disappear as $\Lambda^2/M^2 \rightarrow \infty$. The diagrams contributing to $\Pi_{\mu\nu}^{(0)-1}$ [i.e., the $1/M^2$ term in Eq. (3.13)] with up

$$\begin{aligned}
 \text{---} \circ \text{---} &= \frac{1}{8e^2 \delta_d(0)^2} \\
 \text{---} \circ \text{---} &= -\frac{1}{16M^2 e^2 \delta_d(0)^3} \\
 \text{---} \circ \text{---} &= \text{---} \circ \text{---} = \frac{1}{32M^4 e^2 \delta_d(0)^4}
 \end{aligned}$$

FIG. 6. Vertices with one fermion loop, and $2\kappa + 2$ photon legs. These vertices go as $e^{-2}M^{-2\kappa}$.

to three photon lines are given in Fig. 7. Except for the last two of the three-line diagrams, which are proportional to $D^{-1}(x,y)^3$, all these diagrams are local and proportional to $\delta_{\mu\nu}/M^2$. Consequently, the $1/M^2$ series is

$$\tilde{\Pi}_{\mu\nu}^{(0)-1} = (\delta_{\mu\nu}/M^2) \sum_{n=0}^{\infty} a_n(d)(\Lambda^2/M^2)^n, \quad (4.1)$$

where the contributions to $a_n(d)$ contain exactly n internal photon lines. We would like evidence that this series extrapolates to zero. The diagrams

which contribute to $1/e^2$ contain one fermion loop and n internal photon lines at order $(\Lambda^2/M^2)^n$, leading to a series

$$\tilde{\Pi}_{\mu\mu}^{(1)-1} = \pi \sum_{n=0}^{\infty} b_n(d)(\Lambda^2/M^2)^n \quad (4.2)$$

which should extrapolate to π .

First let us look at the terms proportional to $1/e^2$ since these determine the photon mass. The diagrams up to order Λ^4/M^4 in Eq. (4.2) (two

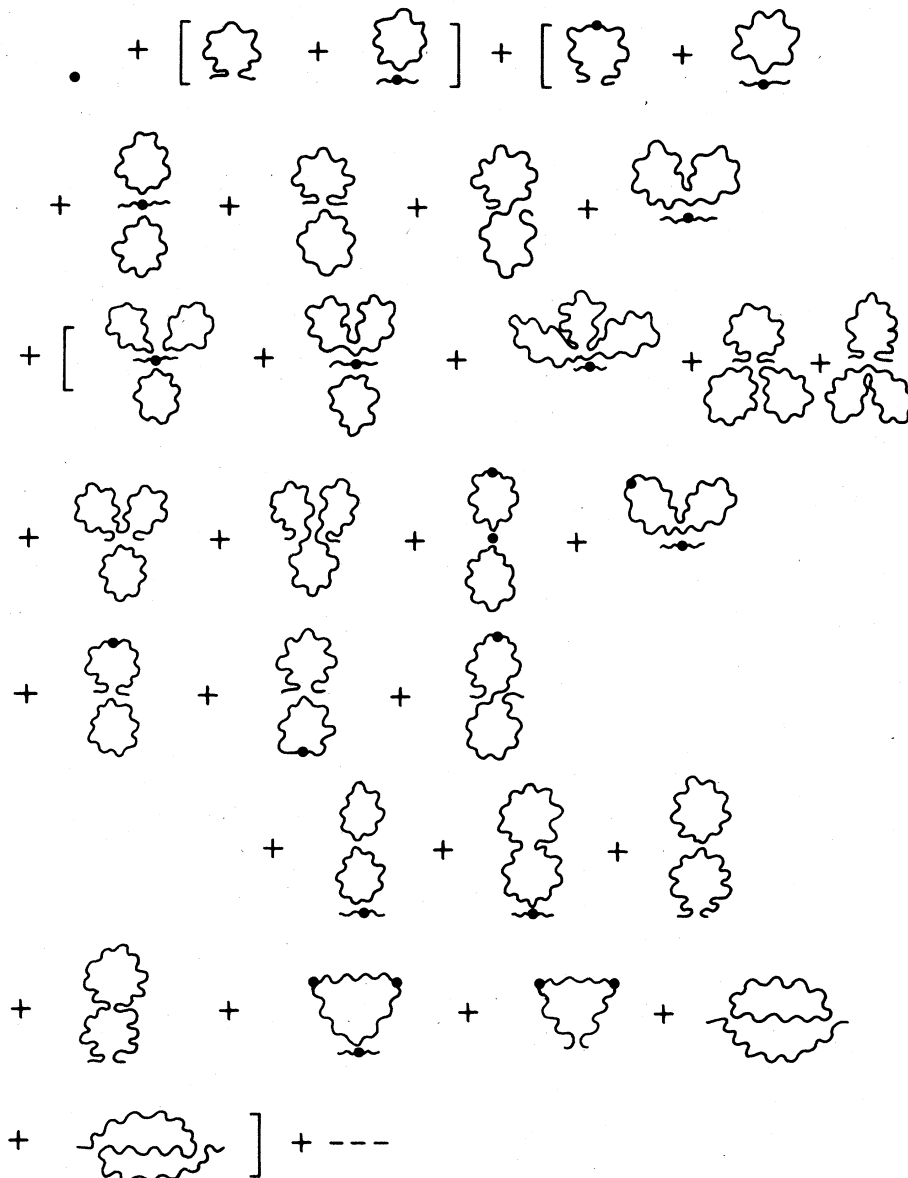


FIG. 7. Diagrams contributing to $\Pi_{\mu\nu}^{(0)-1}$ up to three bare photon inverse propagator lines. Except for the last two diagrams these are proportional to $\delta_{\mu\nu}/M^2$.

internal photon lines) are shown in Fig. 8. As mentioned in the previous section, instead of using smeared vertices we may use the local vertices in Eq. (3.15) provided we multiply the regulated inverse propagators in momentum space by $e^{-p^2/2\Lambda^2}$ as in Eq. (3.3). Consequently, the building blocks for the calculation are

$$\begin{aligned} \tilde{S}^{-1}(p; \Lambda) &= i \not{p} e^{-3p^2/4\Lambda^2}, \\ \tilde{S}^{-1}(x, 0; \Lambda) &= \frac{-2\Lambda^2 \delta_\Lambda(0)}{3^{1+d/2}} \not{x} e^{-\Lambda^2 x^2/3} \end{aligned} \quad (4.3)$$

$$\tilde{D}^{-1}_{\mu\nu}(p; \Lambda) = (g p_\mu p_\nu - \delta_{\mu\nu} p^2) e^{-3p^2/4\Lambda^2}$$

$$\begin{aligned} \tilde{D}^{-1}_{\mu\nu}(x, 0; \Lambda) &= \frac{2\Lambda^2 \delta_\Lambda(0)}{3^{1+d/2}} \left[(2\Lambda^2/3)(\delta_{\mu\nu} x^2 - g x_\mu x_\nu) \right. \\ &\quad \left. + (g-d)\delta_{\mu\nu} \right] e^{-\Lambda^2 x^2/3}. \end{aligned}$$

The basic fermion loop is

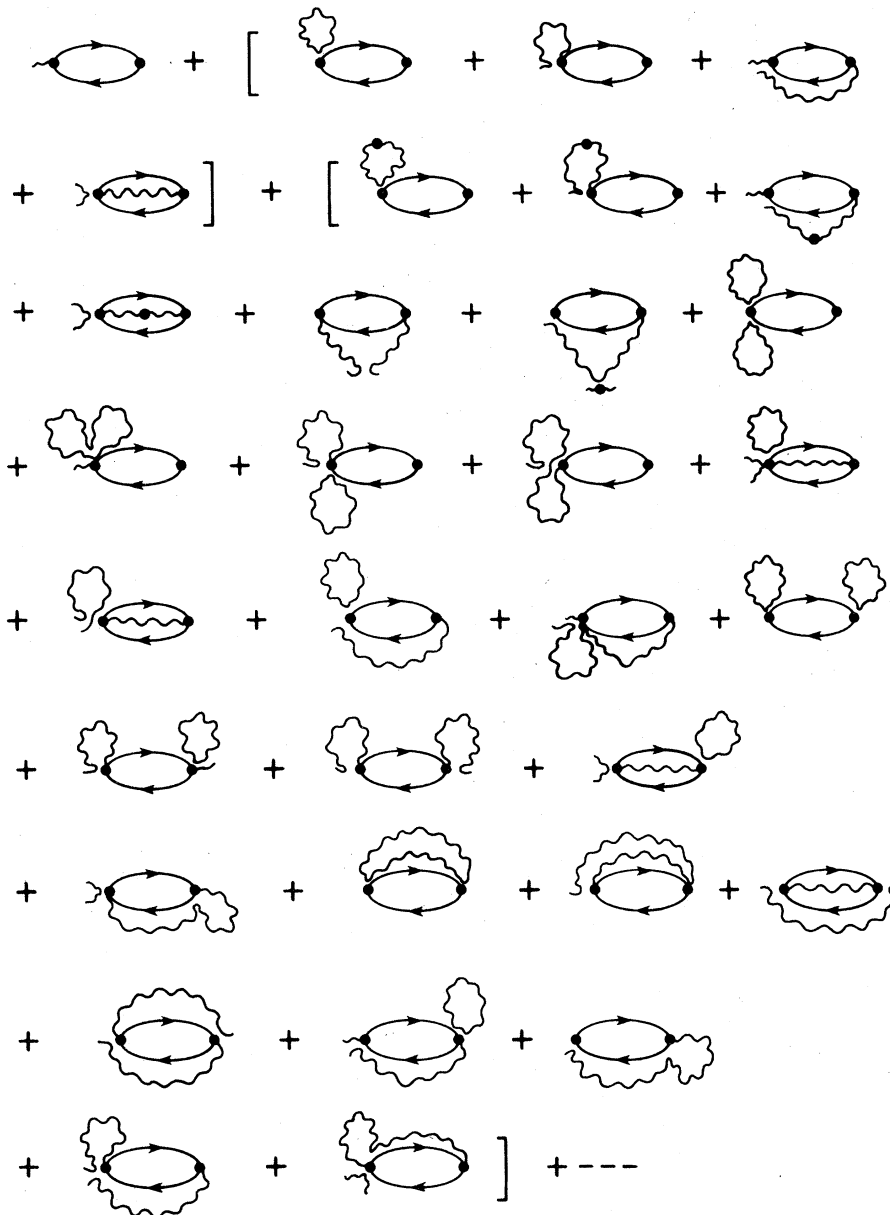


FIG. 8. Diagrams contributing to the first three orders in Λ^2/M^2 in the $1/e^2$ term in $\Pi_{\mu\nu}^{-1}$ [see Eq. (4.2)].

$$\begin{aligned} \text{Tr}[\gamma_\mu \tilde{S}^{-1}(x,0;\Lambda) \gamma_\nu \tilde{S}^{-1}(0,x;\Lambda)] \\ = \frac{2^{2+d/2} \Lambda^4 \delta_\Lambda(0)^2}{3^{d+2}} (\delta_{\mu\nu} x^2 - 2x_\mu x_\nu) e^{-2\Lambda^2 x^2/3}. \end{aligned} \tag{4.4}$$

Fourier transforming and multiplying by the vertex squared we obtain, at zero momentum for the lowest-order diagram of Fig. 8,

$$(1/e^2) \tilde{\Pi}_{\mu\nu}^{(1)-1}(k^2=0) = \frac{(d-2)\delta_{\mu\nu}}{(12)3^{d/2}e^2} \frac{\Lambda^2}{\delta_\Lambda(0)}. \tag{4.5}$$

Since, using Eq. (2.9) near $d=2$,

$$\Lambda^2 = \pi \delta_\Lambda(0) \tag{4.6}$$

$$(1/e^2) \tilde{\Pi}_{\mu\mu}^{(1)-1}(k^2=0) = \pi/e^2 [d(d-2)/36 + f_1(d,g)z + f_2(d,g)z^2 + \dots], \tag{4.7}$$

where

$$z \equiv \Lambda^2/M^2 \tag{4.8}$$

and

$$f_1(d,g) = \frac{d(d+2)}{162 \times 3^{3d/2}} [3^{2+d/2}(d-2)g + 2^{3+d/2}(d-1)g - 3^{2+d/2}d(d-2) - 2^{2+d/2}(d-1)(d-2)], \tag{4.9}$$

$$\begin{aligned} f_2(d,g) = & -\frac{d(d-2)(3d^2+16d+20)(g-d)^2}{108 \times 3^{3d/2}} \\ & -\frac{d(d+2)}{1728 \times 3^{3d/2} 2^{d/2}} (d^2g^2 + 34dg^2 - 56g^2 - 66d^2g + 124dg - 16g + 27d^3 - 84d^2 + 84d - 48) \\ & + \frac{2^{2+d/2}(d-1)d(d+2)^2(3g^2-6g+2d-4)}{675 \times 3^d \times 5^{d/2}} + \frac{(d-2)d(d+2)^2(g^2-2g+d)}{2^{1+d/2} 3^{3+d}} \\ & - \frac{2^{1+d/2}(d-1)(d+2)(3d+10)(g-d)(2g-d+2)}{243 \times 3^{2d}}. \end{aligned} \tag{4.10}$$

$g=1$ is the “natural” Lorentz gauge when there is a photon mass. In order to extrapolate (4.7) to $z=\infty$ we first observe that at $d=2$ we can drop the first term since it is not singular for $z=\infty$. For small z we can replace (4.7) by the [1,1] Padé approximant which has a finite limit as $z \rightarrow \infty$,

$$(1/e^2) \tilde{\Pi}_{\mu\mu}^{(1)-1}(k^2=0) = (\pi/e^2) f_1(d,g)z \left[1 - \frac{f_2(d,g)z}{f_1(d,g)} \right]^{-1} + \dots \xrightarrow{z \rightarrow \infty} -(\pi/e^2) \frac{f_1(d,g)^2}{f_2(d,g)}. \tag{4.11}$$

we find that this diagram goes as $(\pi/e^2)(d-2) \times \delta_{\mu\nu}/36$ for $d \cong 2$. Thus, the factor π in the photon mass squared is just related to phase space in two dimensions. We notice that this diagram formally vanishes as $d \rightarrow 2$. However, higher-order diagrams having n internal photon lines will behave as $(\Lambda^2/M^2)^n$. So, if we could sum the whole series we expect to obtain $(d-2)f(\Lambda^2/M^2)$, where f goes as $1/(d-2)$ times a finite piece as $\Lambda^2/M^2 \rightarrow \infty$. Not being able to do this exactly, we must use Padé approximants to replace the truncated series obtained at a finite order in perturbation theory by a ratio of polynomials which has a limit as $\Lambda^2/M^2 \rightarrow \infty$.

Taking the trace of all the diagrams in Fig. 8 and Fourier transforming at zero momentum we obtain

It is remarkable that if we directly evaluate the right-hand side of Eq. (4.11) for $g=1$ at $d=2$ we obtain

$$\frac{f_1(2,1)^2}{f_2(2,1)} = 0.664 \quad (4.12)$$

which corresponds to a *negative* mass squared. The explanation for this is that f_1 and f_2 are rapidly varying near $d=2$. Hence the necessity of dimensional continuation. In fact, $f_1(d,1)$ has exactly one zero for positive d and that is at $d=2.42$. $f_2(d,1)$ has exactly two zeros for positive d at $d=2.18$ and $d=1.77$. Thus the double zero in the numerator of Eq. (4.12) is about 20% away from $d=2$, while the two zeros in the denominator are on either side of $d=2$ about 10% away. We expect that when higher-order terms are included the zeros in the corresponding polynomials will get closer and closer to $d=2$. A sensible estimate for the photon mass can only be achieved by taking into account the approximate cancellation of these zeros. Thus, we factor them out of Eq. (4.12) to get

$$\frac{f_1(d,1)^2}{f_2(d,1)} = \frac{(d-2.42)^2}{(d-1.77)(d-2.18)} \frac{\tilde{f}_1(d,1)^2}{\tilde{f}_2(d,1)} \quad (4.13)$$

$\tilde{f}_1^2/\tilde{f}_2$ is smoothly behaved for $1 \leq d \leq 4$ and has the value -0.1 at $d=2$. Thus, we see that, just as in weak coupling, the poles at $d=2$ corresponding to the ultraviolet divergence as $\Lambda \rightarrow \infty$ cancel the zero coming from the trace at $d=2$.

The reason the cancellation of zeros is not exact in strong-coupling is twofold. Firstly, we do not sum the series exactly before taking $\Lambda \rightarrow \infty$ but only extrapolate a finite number of terms (here two). Secondly, we expect in low orders contributions from diagrams that would actually go to zero at $d=2$ if we could sum them to all orders. What

is remarkable is that there are exactly the right number of zeros in the numerator and denominator in Eq. (4.13). f_2 is more complicated than a sixth-order polynomial and could easily have had many zeros. Also, assuming that the zeros cancel makes the sign of the square of the photon mass physically acceptable. The “residue” function gives $0.1 \pi/e^2$ for the $O(1/e^2)$ contribution to $\Pi_{\mu\mu}^{-1}$ of Eq. (3.13). This is rather low but not surprising because we have used only the first extrapolant due to the vanishing of the first term in Eq. (4.9).

We expect that higher orders in $1/e^2$ behave in much the same way, i.e., if we could calculate many more terms in the coefficients of $(M^2/e^2)^n$, after removing the cutoff and canceling approximate factors of $(d-2)$, that the series would be recognizable as summing to $1/(e^2/\pi + M^2)$. Only after summing the series could we take the limit $M \rightarrow 0$. This would require a much bigger calculational effort than that presented above. At our level of calculation (up to three photon lines), making use of the Dyson equation and its solution Eq. (3.7), the transverse part of the photon propagator is

$$D_T(k) = \frac{1}{k^2 + (0.1\pi/e^2)^{-1}} \quad (4.14)$$

Going to Minkowski space ($k^2 \rightarrow -k_{\text{Minkowski}}^2$) we obtain a pole at $k_{\text{Minkowski}}^2 = 10e^2/\pi$.

Several times we have mentioned that at higher orders we expect more terms to be proportional to $(d-2)$ so that the pole and zero cancellation will be more exact. An indication of this effect comes from a different calculation of $\Pi_{\mu\nu}^{-1}$ which we performed using a sharp Euclidean cutoff on the d -dimensional momentum-space loop integrals. With this cruder cutoff the results depend on how one routes the momenta for multiloop diagrams, and there exists a routing for which all diagrams at order $1/e^2$ are proportional to $(d-2)$. Explicitly, the result is ($g=1$)

$$\Pi_{\mu\mu}^{(1)-1} = (\pi/e^2)(2-d) \left[1 - 2(d-1)z + \frac{(d-1)(9d^4 + 67d^3 + 102d^2 - 232d - 432)z^2}{4(d+2)^2(d+4)} \right] \quad (4.15)$$

The z term now has a zero at $d=2$ and the z^2 term has two zeros, one at $d=2$ and one at $d=1.833$. After using Padé extrapolants we obtain $(\pi/e^2)[(d-2)/(d-1.833)]1.32$, so that the residue is close to the correct answer of one. The crude cutoff (which is ambiguous precisely because

it depends on how one routes the loop momenta) leads to a pole at $k_{\text{Minkowski}}^2 = 0.76e^2/\pi$.

At the level $(1/e^2)(\Lambda^2/M^2)^3$ there are over one hundred diagrams and it is important to show that the sequence of Padé approximants is converging to the exact answer (one). This work is in progress.

One of the prices paid in performing strong-coupling expansions in a non-gauge-invariant manner is that our procedure for removing the cut-offs Λ, M , gives only a sequence of extrapolants to the true strong-coupling expansion. At any finite order one expects non-gauge-invariant terms in the extrapolants that eventually go to zero as the order increases. To investigate this we turn our attention to the tadpole graphs contributing to $\delta_{\mu\nu}/M^2$ in the cutoff theory which should not exist in the continuum theory [see Eq. (3.12) and subsequent discussion]. Indeed, we find that we can Borel sum an infinite subset of these graphs and that they vanish as $\Lambda^2/M^2 \rightarrow \infty$ independent of the gauge g and type of regulation scheme (Gaussian or θ function). However, when we calculate only the first five terms in the series and extrapolate them to $\Lambda^2/M^2 = \infty$ we find contributions which only slowly go to zero with the order of calculation. This, we believe, is the reason for the rather poor result for the residue function in the previous calculation of the photon mass.

If we look at the purely photonic terms proportional to $\delta_{\mu\nu}/M^2$ coming from the functional determinant

$$K_A \exp \left[\int d^d x \delta_\Lambda(0) \ln \left[1 + \frac{J_s^2}{2M^2 \delta_\Lambda(0)} \right] \right] \tag{4.16}$$

we obtain the set of graphs in Fig. 7. The subset of graphs which contain only $\tilde{D}^{-1}_{\mu\nu}(0,0;\Lambda)$ to various powers can be Borel summed. The vertices are given by [see (3.16)]

$$\delta_\Lambda(0) \ln \left[1 + \frac{J^2}{2M^2 \delta_\Lambda(0)} \right] = \sum_{n=1}^{\infty} L_{2n}/n!(J^2/2)^n, \tag{4.17}$$

where

$$\begin{aligned} L_{2n} &= AB^{n-1}(n-1)!, \\ A &= 1/M^2, \\ B &= \frac{-1}{M^2 \delta_\Lambda(0)}. \end{aligned} \tag{4.18}$$

In any gauge, $\tilde{D}^{-1}_{\mu\nu}(0,0;\Lambda) = \kappa(g, \Lambda) \delta_{\mu\nu}$. For a Gaussian cutoff [Eq. (4.3)]

$$\kappa_G = \frac{2M^2 \delta_\Lambda(0)}{3^{1+d/2}} (g-d) \Lambda^2/M^2, \tag{4.19}$$

whereas for a θ -function cutoff [Eq. (A6)]

$$\kappa_\theta = \frac{M^2 \delta_\Lambda(0)}{d+2} (g-d) \Lambda^2/M^2. \tag{4.20}$$

The result of summing the diagrams in Fig. 9 is

$$(\delta_{\mu\nu}/M^2) [1 + B\kappa(1+d/2) + 2!(B\kappa)^2(1+3d/4+d^2/8) + 3!(B\kappa)^3(1+11d/12+d^2/4+d^3/48) + \dots]. \tag{4.21}$$

At fixed order in $(B\kappa)^n$ the d^n term comes from the diagrams with $(\tilde{D}^{-1}_{\mu\nu})^n$ and is equal to $n!d^n/(2^n n!)$. Thus, for large d we can sum the series to obtain

$$\frac{\delta_{\mu\nu}}{M^2(1-dB\kappa/2)} = \frac{\delta_{\mu\nu}}{M^2[1+(d/2)C(g-d)\Lambda^2/M^2]}, \tag{4.22}$$

where C is a constant which depends on the regulation scheme,

$$C_G = \frac{2}{3^{1+d/2}}, \quad C_\theta = \frac{1}{d+2}. \tag{4.23}$$

Thus, for large d the tadpoles sum to zero independent of the gauge g and method of regulation. In fact, the series can be summed for arbitrary d . It is

$$\delta_{\mu\nu}/M^2 = \sum_{n=0}^{\infty} P_n(d)(B\kappa)^n, \tag{4.24}$$

where

$$P_n(d) = (n+d/2)P_{n-1}(d), \quad P_0(d) = 1, \tag{4.25}$$

so that

$$P_n(d) = \frac{\Gamma(n+d/2+1)}{\Gamma(d/2+1)}. \tag{4.26}$$

Introducing the integral representation of the Γ function, (4.24) becomes

$$\frac{\delta_{\mu\nu}}{M^2} \frac{1}{\Gamma(d/2+1)} \sum_{n=0}^{\infty} (B\kappa)^n \int_0^{\infty} dx e^{-x} x^{n+d/2} = \frac{\delta_{\mu\nu}}{M^2} \frac{1}{\Gamma(d/2+1)} \int_0^{\infty} dx \frac{e^{-x} x^{d/2}}{[1+C(g-d)(\Lambda^2/M^2)x]} \quad (4.27)$$

At $d=2$ we can ask how fast the partial sums of the series (4.24) extrapolate to zero. Calling $B\kappa \equiv y$, so that we are interested in $y \rightarrow \infty$, the series is $(\delta_{\mu\nu}/M^2)f(y)$, where

$$f(y) = 1 + 2y + 6y^2 + 24y^3 + 120y^4 + 720y^5 + \dots \quad (4.28)$$

To obtain estimates at $y = \infty$ we first map $[0, \infty)$ onto $[0,1)$ via¹⁴

$$y = (1/6)z/(1-z) \quad (4.29)$$

to obtain

$$f(z) = 1 + z/3 + z^2/2 + 7z^3/9 + 34z^4/27 + 115z^5/54 + \dots \quad (4.30)$$

This allows us to study the diagonal and off-diagonal Padé sequences at $z=1$. The diagonal sequence is

$$P[0,0]=1, P[1,1]=\frac{1}{3}, P[2,2]=\frac{1}{6} \quad (4.31)$$

and the off-diagonal sequences are

$$\delta_{\mu\nu} A \times \quad \text{---} \quad (1)$$

$$\delta_{\mu\nu} (AB\kappa) \times \quad \text{---} \quad (1), \quad \text{---} \quad \left(\frac{d}{2}\right)$$

$$\delta_{\mu\nu} (2AB^2\kappa^2) \times$$

$$\text{---} \quad \left(\frac{d^2}{8}\right), \quad \text{---} \quad \left(\frac{d}{2}\right), \quad \text{---} \quad (1), \quad \text{---} \quad \left(\frac{d}{4}\right)$$

$$\delta_{\mu\nu} (3!AB^3\kappa^3) \times$$

$$\text{---} \quad \left(\frac{d^3}{48}\right), \quad \text{---} \quad \left(\frac{d^2}{8}\right), \quad \text{---} \quad \left(\frac{d}{6}\right),$$

$$\text{---} \quad \left(\frac{d^2}{8}\right), \quad \text{---} \quad \left(\frac{d}{4}\right), \quad \text{---} \quad \left(\frac{d}{2}\right), \quad \text{---} \quad (1)$$

FIG. 9. Tadpole graphs contributing to $\delta_{\mu\nu}/M^2$ proportional to $(B\kappa)^n$, where $\bar{D}_{\mu\nu}^{-1(0)} = \kappa\delta_{\mu\nu}$, $B = -M^{-2}/\delta_{\Lambda}(0)$.

$$\begin{aligned}
 P[1,2] &= 0.4348, & P[2,3] &= 0.21264, \\
 P[2,1] &= 0.4333, & P[3,2] &= 0.21268.
 \end{aligned}
 \tag{4.32}$$

Each sequence appears to be approaching zero, but even with six terms in the series there is a non-negligible contribution to a term which must vanish as $\Lambda^2/M^2 \rightarrow \infty$. So, non-gauge-invariant tadpoles exist at finite order and, in our extrapolation scheme, only go away if the calculation is carried to very high orders. This is the price we must pay for using a non-gauge-invariant cutoff in order to expand about the formal local potential energy of QED.

V. CONCLUSIONS

We have formulated a strong-coupling expansion for QED in d -dimensional Euclidean space. A continuum UV regulation is adopted because this ensures the correct fermionic spectrum, without violating chiral symmetry. We concentrate on a Gaussian cutoff at large momentum since this is soft enough to allow for straightforward evaluation of all multiloop integrals. As a consequence both the kinetic and potential terms in the action are nonlocal and violate gauge invariance. In addition a photon mass must be included as an infrared (IR) cutoff.

In order to handle this violation of gauge invariance, it is necessary to continue the theory into arbitrary space-time dimension. There strong-coupling calculations for the cutoff theory may be carried out and the cutoff removed prior to returning to the integer dimension of interest. As an example we calculate the photon propagator in the two-dimensional theory. There we find many strong-coupling diagrams are proportional to $d-2$ (from traces over fermion loops) times highly divergent integrals. It is possible for infinite sums of such integrals to conspire to produce poles at $d=2$ which cancel the zero from the trace, giving a finite result. Of course, inasmuch as it is only practical to calculate a finite number of terms in the strong-coupling expansion the extrapolants will have poles only approximately at dimension 2. Nevertheless, it is essential to take into account this approximate cancellation if realistic answers are to be obtained.

Our strong-coupling expansion for the inverse photon self-energy in two dimensions involves a gauge-dependent term inversely proportional to the IR regulator mass. A subclass of diagrams contri-

buted to this term may be summed to all orders and shown to vanish as the UV cutoff is removed. However, the corresponding sequence of extrapolants converges only slowly to zero. We take this to be the reason why low-order calculations of the photon mass are numerically inaccurate.

Higher-order calculations are needed to unambiguously test the restoration of gauge invariance. The low-order calculations presented here indicate that the violation of gauge invariance in continuum regulated theories may not be serious and that a consistent strong-coupling expansion for fermions coupled to gauge fields which preserves chiral symmetry and the correct number of fermion degrees of freedom is possible.

ACKNOWLEDGMENTS

The Borel summation of subclasses of diagrams was done in collaboration with Carl Bender. We thank him together with Peter Carruthers, Gerald Guralnik, Dean Preston, Ralph Roskies, and David Sharp for helpful conversation. Finally, we thank the MIT Mathlab for the use of MACSYMA.

APPENDIX: THE REGULATION OF DIAGRAMS IN d DIMENSIONS

In our work on $g\phi^4$ field theory¹⁻⁴ we espoused a lattice regulation of the Dirac δ function so as to easily evaluate the strong-coupling diagrams. We used¹¹

$$\delta(x-y) \rightarrow \delta_{\text{latt}}(x-y) = \delta_{ij}/a^d \equiv \delta_0/a^d, \tag{A1}$$

where a is the lattice spacing, so that

$$\begin{aligned}
 \partial^2 \delta_{\text{latt}}(x-y) &= (1/a^{2+d}) \\
 &\times \left[- \sum_{\mu=1}^d (\delta_{+\mu} + \delta_{-\mu}) + 2d\delta_0 \right]. \tag{A2}
 \end{aligned}$$

However, such a definition is quite awkward when dealing with vector particles because of difficulties with the restoration of rotational invariance. It also causes state doubling if the inverse fermion propagator is taken to be

$$\not{\partial} \delta_{\text{latt}}(x-y) = (1/a^{1+d}) \sum_{\mu=1}^d \gamma_{\mu} (\delta_{+\mu} - \delta_{-\mu}). \tag{A3}$$

Consequently, it is preferable to work in the continuum.

The procedure used in this paper is to softly cut-off the δ function using a Gaussian, Eq. (1.1). The result is that all inverse propagators are smoothly cut off at large momenta. In addition, the vertices of the strong-coupling expansion must be smeared using the regulated δ function for the reasons discussed in Ref. 11. This can be translated into the use of local vertices together with a modified momentum cutoff on internal lines. It is easiest to evaluate multiloop diagrams in coordinate space. Then all integrals amount to nothing more complicated than the Fourier transform of a polynomial times a Gaussian. In fact, all the algebra and integrations can be performed using routines available on MACSYMA.

An alternative continuum regulation was introduced in Ref. 11. It is a sharp θ -function cutoff in momentum space,

$$\delta(p) \rightarrow \delta_\Lambda(p) = \theta(\Lambda - |p|), \quad (\text{A4})$$

and has the advantage over the Gaussian of

$$S^{-1}(x; \Lambda) = \partial \delta_\Lambda(x) = -\Lambda / (2\pi |x|)^{d/2} (\Lambda x / |x|) J_{1+d/2}(\Lambda |x|) \quad (\text{A7})$$

and

$$\begin{aligned} D^{-1}_{\mu\nu}(x; \Lambda) &= (\delta_{\mu\nu} \partial^2 - g \partial_\mu \partial_\nu) \delta_\Lambda(x) \\ &= \left[\frac{\Lambda}{2\pi |x|} \right]^{d/2} \Lambda^2 \left\{ \delta_{\mu\nu} \left[\frac{g+2}{\Lambda |x|} J_{1+d/2}(\Lambda |x|) - J_{d/2}(\Lambda |x|) \right] \right. \\ &\quad \left. - \frac{g x_\mu x_\nu}{x^2} \left[\frac{d+2}{\Lambda |x|} J_{1+d/2}(\Lambda |x|) - J_{d/2}(\Lambda |x|) \right] \right\} \quad (\text{A8}) \end{aligned}$$

in coordinate space, and

$$S^{-1}(p; \Lambda) = -i \not{p} \theta(\Lambda - |p|) \quad (\text{A9})$$

and

$$D^{-1}_{\mu\nu}(p; \Lambda) = (g p_\mu p_\nu - \delta_{\mu\nu} p^2) \theta(\Lambda - |p|) \quad (\text{A10})$$

in momentum space. Obviously, one-loop integrals

preserving the convolution property

$$\delta_\Lambda(p)^2 = \delta_\Lambda(p). \quad (\text{A5})$$

In d -dimensional coordinate space Eq. (A4) becomes

$$\delta_\Lambda(x) = J_{d/2}(\Lambda |x|) \left[\frac{\Lambda}{2\pi |x|} \right]^{d/2}. \quad (\text{A6})$$

We also saw in Ref. 11 that (A6) led to convergent sequences of approximants, whereas for the Gaussian scheme the sequence of approximants was asymptotic. Although these facts suggest that a θ -function cutoff is preferable, calculations requiring dimensional continuation are complicated by the Bessel function appearing in Eq. (A6).

Smearing of the strong-coupling vertices is again necessary, but does not translate into a modified cutoff on internal lines when local vertices are used because of Eq. (A5). The inverse free propagators are

are easiest in momentum space. But, in general, multiloop integrals can only be evaluated by Fourier transforming the products of Bessel functions which appear in the coordinate representation. The two-loop integrals which appear in the Schwinger-model calculation can be done analytically. For higher orders numerical methods must be used. The calculation will be reported in a forthcoming paper.

¹C. M. Bender, F. Cooper, G. S. Guralnik, and D. H. Sharp, Phys. Rev. D **19**, 1865 (1979). See also S. Hori, Nucl. Phys. **30**, 644 (1962); G. Heber and H. J. Kaiser, Z. Naturforsch. **19a**, 828 (1964); B. F. L. Ward, Nuovo Cimento **45A**, 1 (1978).

²C. M. Bender, F. Cooper, G. S. Guralnik, and D. H. Sharp, in *Recent Developments in High Energy Physics*, edited by Behram Kurşunoğlu, Arnold Perlmutter, and Linda F. Scott (Plenum, New York, 1980).

- ³C. M. Bender, F. Cooper, G. S. Guralnik, H. Moreno, R. Roskies, and D. H. Sharp, *Phys. Rev. Lett.* **45**, 501 (1980).
- ⁴C. M. Bender, F. Cooper, G. S. Guralnik, R. Roskies, and D. H. Sharp, *Phys. Rev. D* **23**, 2976 (1981); **23**, 2999 (1981).
- ⁵K. G. Wilson, in *New Phenomena in Subnuclear Physics*, proceedings of the 14th course of the International School of Subnuclear Physics, Erice, 1975, edited by A. Zichichi (Plenum, New York, 1977); L. Susskind, *Phys. Rev. D* **16**, 3031 (1977).
- ⁶F. Guerin and R. D. Kenway, *Nucl. Phys.* **B176**, 168 (1980).
- ⁷K. G. Wilson, *Phys. Rev. D* **10**, 2445 (1974); J. Kogut and L. Susskind, *ibid.* **11**, 395 (1975).
- ⁸G. 't Hooft and M. Veltman, *Nucl. Phys.* **B44**, 189 (1972).
- ⁹G. Leibbrandt, *Rev. Mod. Phys.* **47**, 849 (1975).
- ¹⁰P. Castoldi and C. Schomblond, *Nucl. Phys.* **B139**, 269 (1978).
- ¹¹C. Bender, F. Cooper, R. D. Kenway, and L. M. Simons, preceding paper, *Phys. Rev. D* **24**, 2693 (1981).
- ¹²J. Schwinger, *Phys. Rev.* **128**, 2425 (1962).
- ¹³K. Johnson, in *Lectures on Particles and Field Theory*, Brandeis Summer Institute, edited by S. Deser (Prentice Hall, New Jersey, 1965), Vol. 2. See Eq. (3.17) for a correct gauge-invariant expression for $\Pi_{\mu\nu}(p)$ in four dimensions.
- ¹⁴This Euler transform was used to analyze the high-temperature series for $g\phi^4$ field theory. See G. A. Baker, Jr. and John M. Kincaid, *J. Stat. Phys.* **24**, 469 (1981).